Pakistan Veterinary Journal

ISSN: 0253-8318 (PRINT), 2074-7764 (ONLINE)
DOI: 10.29261/pakvetj/2026.144

RESEARCH ARTICLE

Genomic Characterization of Plasmid-Mediated *tet*(X4), *mcr-1*, and *bla*$_{NDM-5}$ Genes in *Escherichia coli* from Farmed Minks Highlights Their Role as a One Health Reservoir

Asim Munir[1#], Muhammad Shoaib[1#], Yuetong Lv[1], Ruilong Song[1], Edward J Feil[2], Zhiqiang Wang[1,3,4,5]* and Ruichao Li[1,3,4,5]*

[1]Jiangsu Co-innovation Center for Prevention and Control of Important Animal Infectious Diseases and Zoonoses, College of Veterinary Medicine, Yangzhou University, Yangzhou, P. R. China; [2]The Milner Centre for Evolution, University of Bath, Claverton Down, Bath BA2 7AY, UK; [3]Jiangsu Interdisciplinary Center for Zoonoses and Biosafety, Yangzhou University, Yangzhou, 225009, PR China; [4]Institute of Comparative Medicine, Yangzhou University, Yangzhou, P. R. China; [5]Jiangsu Key Laboratory of Zoonosis, Yangzhou University, Yangzhou, 225009, PR China.
# These authors equally contributed to this study.
*Corresponding author: rchl88@yeah.net (RL); zqwang@yzu.edu.cn (ZW)

ARTICLE HISTORY (26-290)

Received: March 27, 2026
Revised: April 19, 2026
Accepted: June 21, 2026
Published online: June 25, 2026

Key words:
bla$_{NDM-5}$
Escherichia coli
mcr-1
Minks
Plasmid mediated
tet(X4)

ABSTRACT

The emergence and dissemination of plasmid-mediated resistance to tigecycline, colistin, and carbapenems in *Escherichia coli* pose a serious public health threat. This study intended to reveal the genomic characteristics of *E. coli* isolates resistant to these last-resort antibiotics recovered from minks. A total of 100 samples were collected from 25 farmed minks obtained post-slaughter from a single commercial fur farm, with four tissue types sampled per animal including liver, lungs, spleen, and intestine. Following phenotypical characterization all resistant isolates were characterized by Illumina short-read whole-genome sequencing and six representative isolates were further subjected to CycloneSEQ long-read sequencing to reveal complete genomic profile. Conjugation and fitness cost assays were employed to evaluate the transfer rate and biological burden of resistance genes. Collectively, 25 *E. coli* isolates were recovered that harbor one or more plasmid-mediated antimicrobial resistance genes *mcr-1*, *tet*(X4), or *bla*$_{NDM-5}$, imparting resistance to colistin, tigecycline, and carbapenems, respectively. Among these, *mcr-1*-positive isolates accounted for 52% (n=13), while *tet*(X4), and *bla*$_{NDM-5}$ were each detected in 24% (n=6) isolates. The resistant *E. coli* strains exhibited diverse sequence types, predominantly ST746, ST219, and ST641.The *tet*(X4) gene was located on ~190kb hybrid IncFIA (HI1)/HI1B(R27)/HI1A plasmid, whereas *mcr-1* and *bla*$_{NDM-5}$ were associated with IncI2, IncX4, IncHI2, and IncX3, IncB/O/K/Z plasmid types respectively. Moreover, the virulence profile revealed that all *E. coli* isolates belong to ExPEC (UPEC) pathotype. At present, this study represents the first identification of *tet*(X4)-positive *E. coli* and carbapenem-resistant *bla*$_{NDM-5}$-positive *E. coli* coexisting with colistin resistant *mcr-1* gene from minks in China. This study emphasizes the need of continued surveillance to observe the pervasiveness and dissemination of emerging ARGs in minks.

To Cite This Article: Munir A, Shoaib M, Lv Y, Song R, Feil EJ, Wang Z and Li R, 2026. Genomic characterization of plasmid-mediated *tet*(x4), *mcr-1*, and *bla*$_{ndm-5}$ genes in *Escherichia coli* from farmed minks highlights their role as a one health reservoir. Pak Vet J, 46(6): 1525-1535. http://dx.doi.org/10.29261/pakvetj/2026.144

INTRODUCTION

In recent years, the global spread of antimicrobial resistance (AMR) has emerged as a major public health crisis (Tang *et al*., 2023). The escalating burden of bacterial multidrug resistance (MDR) has coincided with an increase in the use of veterinary antibiotics for therapeutic and prophylactic management in food-producing animals (Biswas *et al*., 2022). Historically, antimicrobials were routinely administered at sub-therapeutic concentrations as growth promoters in livestock. The increase of MDR is not limited to the veterinary sector; irrational prescribing practices in clinical medicine also increase selection pressure favoring the emergence of resistant pathogens. The dissemination of clinically relevant MDR bacteria in wildlife

increasingly recognized as dynamic bio-indicators for AMR surveillance (Ramey, 2021). The prevalence of AMR within wildlife and broader ecosystems represents a substantial public health threat, particularly as 58% of human pathogens are zoonotic in nature (Qian *et al.*, 2022). Wild animals can act as environmental reservoirs, facilitating the spread of resistant bacteria and ARGs to human populations and domestic livestock (Ahlstrom *et al.*, 2022; Dalazen *et al.*, 2023;Vezeau and Kahn, 2024).

Escherichia coli (*E. coli*) a Gram-negative bacterium that is widely distributed in the intestinal tracts of humans and animals (Munir *et al.*, 2025a). As a commensal microorganism, it plays an important role in maintaining gut microbial homeostasis (Schubert *et al.*, 2025). However, certain strains have acquired multiple virulence factors including adhesion-related genes (*fim*H and *fim*C), iron acquisition systems (*iut*A and *iro*N), and hemolysin genes (*hly*A) and exhibit pronounced pathogenicity (Pakbin, Brück, and Rossen, 2021), that not only threaten animal health but can also spread through the food chain or environmental pathways, posing risks to public health (Ahmed *et al.*, 2025). Moreover, *E. coli* act as an important reservoir and vehicle for ARGs, capable of facilitating horizontal gene transfer (HGT) between clinical and non-clinical ('One-Health') settings (Poirel *et al.*, 2018).

The long-term and excessive use of antibiotics in animal production lead to emergence of , MDR phenotypes (Li *et al.*, 2022) carrying key resistance genes including *mcr* (colistin resistance), bla_{NDM} (carbapenem resistance), $bla_{CTX\text{-}M}$ (extended-spectrum cephalosporin resistance), *tet*(X) (tigecycline resistance) have been widely detected in both animal and human-derived isolates (Lu *et al.*, 2022).

The mink is an important fur-bearing animal in China and serves as a valuable model in studies of animal disease, genetics, and environmental adaptation. Northern China including Shandong, Liaoning, Hebei, and Heilongjiang provinces constitutes the major mink-farming region, and accounts for a large propagation of the minks population in China (Zhang *et al.*, 2015). Intensive farming practices and irrational use antibiotics as growth promotors, or for prophylactic measures, has driven the dissemination of resistant bacterial isolates (Munir *et al.*, 2025b). However, detailed epidemiological and genetic investigations using whole genome sequencing of mink-derived *E. coli* remain very limited. This work aimed to identify and characterize MDR *E. coli* isolates collected from mink farms in China to provide a deeper understanding of the potential public health risks and transmission potential in One Health settings.

MATERIALS AND METHODS

Sample collection and bacterial isolation: A total of 100 samples were collected from 25 apparently healthy mink bodies obtained post-slaughter from a single commercial fur farm for fur production purposes, with four tissue types sampled per animal including liver, lungs, spleen, and intestine in Shandong, China. Each sample was enriched in Brain Heart Infusion (BHI) broth (Oxoid, UK) for18-h incubation at 37℃ followed by inoculation onto MacConkey agar plates separately supplemented with meropenem (2 μg/mL), tigecycline (2 μg/mL), and colistin (2 μg/mL) and incubated overnight at 37℃. Species identification was carried out using MALDI-TOF MS (Bruker Daltonics), and the presence of high-priority resistance genes, specifically *tet*(X), *mcr-1*, and bla_{NDM}, was confirmed through PCR amplification using gene-specific primers as previously reported by Munir *et al.* (2025b).

Antimicrobial susceptibility testing: Antimicrobial susceptibility profiles of the MDR isolates were determined against 8 different antibiotics using the broth micro-dilution method, following Clinical and Laboratory Standards Institute (CLSI) guiding principle and European Committee on Antimicrobial Susceptibility Testing (EUCAST, 2024) (CLSI, 2020). *E. coli* ATCC 25922 served as quality control strain.

Conjugation experiment: To evaluate the horizontal transfer potential and mobility of the plasmid-borne resistance genes *tet*(X4), *mcr-1*, and $bla_{NDM\text{-}5}$, conjugation experiment via surface mating method was performed using rifampicin-resistant *E. coli* C600 as a recipient. We used a protocol described previously (Munir *et al.*, 2025b), with minor amendments. Conjugation frequencies were calculated by dividing the number of transconjugant CFU by the total CFU of recipient bacteria. To confirm the presence of ARGs, PCR amplification was performed using 1μL of the bacterial culture as a template. Isolates harboring target ARGs were sub- cultured onto MacConkey agar to characterize the colony morphology of the transconjugants. All experimental procedures were performed in duplicate.

Growth curve assay: Single bacterial colonies were inoculated into 5 mL LB broth and incubated at 37°C with 200 rpm shaking. To monitor the growth kinetics 200 mL of bacterial culture was added into a 96-well flat-bottom plate whilst uninoculated LB broth was used as a negative control. Bacterial growth kinetics were determined out by measuring the optical density at 600 nm using a spectrophotometer (Thermo Fisher, Waltham, MA, USA) from 0 to 20 h at every 20 minutes. Experiments were performed with three biological replicates (Tang *et al.*, 2022).

In-vitro competition assay: Single colonies of resistant and susceptible reference strain (*E. coli* ATCC 25922) were suspended in 5ml LB broth and incubating in a shaking incubator (200rpm) for 6h at 37°C to obtain logarithmic. The bacterial isolates were then mixed at a ratio of 1:1 and sequentially diluted 10-fold in 0.85% saline solution at 0, 24, 48, and 72 h, before culturing on LB agar plates with or without antibiotics overnight at 37°C. The relative fitness of two strains was calculated by the following formula: Relative fitness (Rf) = ln[R(t)]- ln [R(0)](Tang *et al.*, 2022).

Whole genome sequencing and bioinformatics analysis: Genomic DNA (gDNA) was isolated using the FastPure® DNA Isolation Mini Kit (Vazyme, China). DNA concentration, purity and integrity were assessed by spectrophotometer (Colibri LB 915, Titertek-Berthold,

Germany) and agarose gel electrophoresis. Short read sequencing was carried out for all 25 resistant *E. coli* isolates via Illumina HiSeq2500 platform using a 2×150 bp paired-end configuration. Raw sequences were trimmed to get clean reads using Trimmomatic v0.39 (Bolger, Lohse, and Usadel, 2014) and *de novo* assembly was conducted via SPAdes v4.0 with default parameter (Prjibelski *et al.*, 2020). Multi-locus sequence types were assigned using command line tool (/tseemann/mlst) while resistance gene and plasmid replicon profiles were characterized using ResFinder v4.1 and PlasmidFinder v2.1, respectively (Bortolaia *et al.*, 2020; Carattoli and Hasman, 2020). Virulence genes, phylogroups and serotypes of *E. coli* isolates were determined using the IPEC-ExPEC database, ClermonTyping and ECTyping v1.0 respectively (Beghain *et al.*, 2018; Bessonov *et al.*, 2021). Annotation of the draft genomes were completed using Prokka v1.12 (Seemann, 2014).

However six representative isolates were subjected to long-read sequencing using the CycloneSEQ technologies (Peng *et al.*, 2025) followed by integrating Illumina short-read data with CycloneSEQ long-reads using Unicycler v0.4.8 *de novo* assembler to get complete genomes (Wick *et al.*, 2017). Annotation of the genomes were completed using the Rapid Annotations using Subsystems Technology (RAST) (https://rast.nmpdr.org/rast.cgi) (Overbeek *et al.*, 2014).

Roary v3.13.0 was used for pan genome analysis, and FastTree v2.1.11 for maximum-likelihood phylogenetic tree construction (Price, Dehal, and Arkin, 2009; Page *et al.*, 2015). Snp-dists v0.7.0 was used to determine the single nucleotide polymorphisms (SNPs) distances (https://github.com/tseemann/snp-dists). The tree was visualized using iTOL v5 (https://itol.embl.de/itol.cgi). BRIG v0.95 (Alikhan *et al.*, 2011) and Easyfig v2.2.3 (Sullivan, Petty, and Beatson, 2011) were used to compare data generated in this study with NCBI reference sequences.

RESULTS

Identification and antimicrobial resistance profile of resistant isolates: A total of 25 resistant *E. coli* isolates were recovered from four tissue types, including intestine (n=5), lungs (n=6), liver (n=7), and spleen (n=7). These isolates were obtained from nine minks, with multiple isolates recovered per animal, reflecting intra-host distribution of resistance across different tissue compartments. However, phenotypic and genotypic analysis revealed that 13 isolates (52%) harbored *mcr-1*, six isolates (24%) carried *tet*(X4), and six isolates (24%) carried bla_{NDM-5} gene (Fig 1). Notably, all six (100%) bla_{NDM-5} -positive isolates co-harbored both *mcr-1* and *fosA3* genes, while in case of *mcr-1*-positive isolates only 5/13 (38.4%) isolates co-carried the *fosA3* gene, indicating frequent co-occurrence of these resistance determinants within single isolates. All these isolates (100%) are resistant to ampicillin and kanamycin (MICSs: >128µg/mL and 64 - >128µg/mL, respectively) and displayed modest to high MIC against TET, TIG, CTX, MEM, CST, GEN (Table 2).

Transferability of *tet*(X4), *mcr-1* and bla_{NDM-5} positive *E. coli* isolates: The ARGs bla_{NDM-5}, *mcr-1*, and *tet*(X4) were plasmid-borne. In conjugation assay all bla_{NDM-5} and *mcr-1*-positive *E. coli* isolates successfully transferred resistance to the *E. coli* C600 recipient strain with conjugation frequencies summarized in Table 3. Whereas, repeated attempts with *tet*(X4)-positive isolates failed to produce transconjugants, suggesting limited or non-conjugative transfer under the experimental conditions.

Growth dynamics and fitness impact of resistant *E. coli* Isolates: Notably, most resistance gene-bearing isolates demonstrated decreased growth rates relative to the reference susceptible strain *E. coli* ATCC 25922, although certain isolates (e.g., 11FT, 3CM, 5PC, 11GC) exhibited only minimal growth reduction after 10 hours (Fig 2a–c), indicating that the fitness burden is both strain and gene dependent. Subsequently, fitness cost associated with *tet*(X4), *mcr-1*, and bla_{NDM-5} was evaluated under an antibiotic-free environment to further assess the biological burden imposed by these resistance genes on their respective host strains. All the resistant isolates were competed with susceptible *E. coli* with of CFU/mL ratios (resistant: susceptible) recorded at 24, 48, and 72 h. Consistent with the growth rate data, most of the resistant isolates were less competitive, but some isolates (3PT, 8GT, 3CM, 4PM, 5PC and 10PC) became more moderate at the later stages possibly due to compensatory adaptations. Isolates with dramatically reduced growth (e.g., 12GT, 7FT, 5PM, 5GM, 3FC, 10GC and 8GC) tend to have higher fitness cost but exceptions occur where impact on growth rate does not correlate with a strong on competitive fitness (e.g., 12GT, 5GM and 3FC) (Fig 2). Overall, results suggest that *tet*(X4), *mcr-1* and bla_{NDM-5} genes impose a fitness cost that reduces growth rate and competitiveness against susceptible isolates.

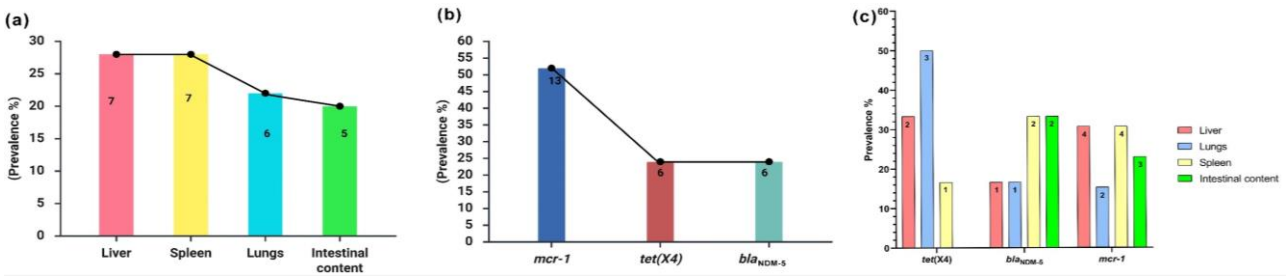

Fig. 1: Prevalence and distribution of antimicrobial resistance genes (ARGs) among *E. coli* isolates recovered from post-slaughter mink carcasses (n = 25 animals: single farm). (a) Prevalence (%) of ARG-positive *E. coli* isolates recovered from different tissue/organ sampling sites. (b) Overall prevalence (%) of *mcr-1*, *tet*(X4), and bla_{NDM-5} resistance genes among ARG-positive isolates. (c) Distribution of individual ARGs across tissue/organ sampling sites; bar heights represent prevalence (%) calculated relative to the total number of ARG-positive isolates, and numbers within bars indicate the corresponding isolate counts (n=25).

Table 1: Genetic characteristics of seven *E. coli* isolates sequenced by Cyclone SEQ followed by hybrid assembly approach

Sample ID	Source	MLST	Component	Replicon types	Size (bp)	ARGs
11FT	lungs	ST 2165	11FT-chromosome	-	3,278,876	*bla*$_{EC-18}$
			p11FT-tetX4	IncFIA (HI1), IncHI1B(R27), IncHI1A	190,697	*tet*(X4), *floR*, *qnrS1*, *lnu*(G), *aadA22*, *bla*$_{TEM-1}$
			p11FT-138kb	IncFII(pSE11)	138,660	*dfrA14*, *sul2*, *aph (3'')-Ib*, *aph(6)-Id*, *bla*$_{TEM-1}$,*tet*(A)
			p11FT-3kb	Col(pHAD28)	3,133	none
			p11FT-3kb-RNAI	ColRNAI	3,667	none
3PT	Spleen	ST 746	3PT chromosome	-	4,602,317	*dfrA12*, *aadA2*, *cmlA1*, *aadA1*, *bla*$_{TEM-1}$, *qnrS1*, *aac(3)-IId*, *sul3*, *bla*$_{EC-15}$
			p3PT-tetX4	IncFIA (HI1), IncHI1B(R27), IncHI1A	190,711	*tet*(X4), *floR*, *qnrS1*, *lnu*(G), *aadA22*, *bla*$_{TEM-1}$
			p3PT-111kb	IncFIB(pHCM2)	111,793	*dfrA51*
			p3PT-46kb	IncX1	46,712	*aph (3')-Ia*, *bla*$_{CTX-M-55}$, *qnrS1*, *tet*(A)
			p3PT-9kb	ColE10	9,981	none
8GC	Intestinal content	ST 136	8GC chromosome	-	4,776,497	*tet*(B), *bla*$_{EC-19}$
			p8GC-152kb	IncFIB (AP001918)	152,191	*aac(3)-IVa*, *sul2*, *floR*, *bla*$_{TEM-1}$, *dfrA12*, *aadA2*, *mph(A)*
			p8GC-fosA3	IncI1-I(Alpha)	106,759	*fosA3*, *bla*$_{CTX-M-14}$
			p8GC-mcr1	IncI2(Delta)	67,138	*mcr-1*
			p8GC-4kb	Col(pHAD28)	4,049	none
11PC	Spleen	ST 641	11PC-chromosome	-	4,767,868	*bla*$_{EC-13}$
			p11PC-mcr1	IncI2(Delta)	68,121	*mcr-1*
			p11PC-110kb	IncB/O/K/Z	110,380	*aph (3')-IIa*, *oqxB*, *oqxA*
			p11PC-91kb	p0111	91,730	*floR*, *tet*(A), *sul2*, *aph (3'')-Ib*, *aph (6)-Id*, *bla*$_{TEM-1}$
			p11PC-191kb	IncFIB (AP001918)	191,321	none
7CC	Intestinal content	ST 973	7CC-chromosome	-	5,135,068	*bla*$_{EC-19}$, *floR*, *tet*(A), *sul2*, *aph (3'')-Ib*, *aph (6)-Id*
			p7CC-fosA3	IncHI2	230,346	*dfrA12*, *aph (3')-Ia*, *bla*$_{CTX-M-14}$, *fosA3*, *sul1*, *bleO*, *oqxA2*, *oqxB2*
			p7CC-118kb	IncFIC (FII)	118,944	*tet*(A), *aph (6)-Id*, *aph (3'')-Ib*, *sul2*, *mph(A)*, *sul1*, *aadA5*, *dfrA17*, *aac(3)-IId*, *bla*$_{TEM-1}$
			p7CC-85kb	IncI1-I(Alpha)	85,892	none
			p7CC-mcr1	IncX4	36,373	*mcr-1*
			p7CC-5kb	ColRNAI	5,891	none
			p7CC-4kb	Col(pHAD28)	4,049	none
			p7CC-1kb	Col (MG828)	1,545	none
3CM	Intestinal content	ST 1011	3CM-chromosome	-	5,101,625	*aac(3)-IId*, *mph(A)*, *bla*$_{TEM-1}$, *bla*$_{EC-15}$
			p3CM-mcr1	IncHI2	180,961	*mcr-1*, *aac(3)-IVa*, *aph(4)-Ia*, *aph(3')-Ia*, *aph(6)-Id*, *aph(3'')-Ib*, *lnu(F) aadA22* , *fosA3*, *bla*$_{TEM-1}$, *dfrA14*, *aadA1*, *bla*$_{OXA-10}$, *cmlA5 arr-2*, *qnrS1*, *tet*(A), *floR*
			p3CM-97kb	p0111	97,926	none
			p3CM-NDM-5	IncX3	46,161	*ble-MBL*, *bla*$_{NDM-5}$
			p3CM-3kb	Col(pHAD28)	3,781	none
			p3CM-3kb	Col (MG828)	3,083	none
4FM	lungs	ST 219	4FM-chromosome	-	5,253,559	*bla*$_{EC-19}$, *erm(B)*
			p4FM-mcr1	IncHI2	373,134	*mcr-1*, *floR*, *aac(3)-IVa*, *aph(4)-Ia*, *aph(3')-Ia*, *aph(6)-Id*, *aph(3'')-Ib*, *lnu(F)*, *aadA22*, *oqxA2*, *oqxB*, *tet*(A), *aph(6)-Id*, *aph(3'')-Ib*, *sul2*, *bla*$_{TEM-1}$, *bleO* ,*sul1*, *bla*$_{CTX-M-65}$
			p4FM-NDM-5	IncB/O/K/Z	113,155	*fosA3*, *dfrA12*, *aadA2*, *sul1*, *ble-MBL*, *bla*$_{NDM-5}$, *aph(3')-Ia*, *mph(A)*
			p4FM-5kb	Col(pHAD28)	5,772	none
			p4FM-5kb	Col156	5,015	none
			p4FM-2kb	Col (MG828)	2,617	none

Table 2: The MICs (μg/mL) of positive *E. coli* isolates against eight antimicrobials

Strain IDs	TET R (≥16)	TIG R (≥0.5)	MEM R (≥4)	CST R (≥4)	AMP R (≥32)	GEN R (≥16)	KAN R (≥64)	CTX R (≥4)
11FT	128	16	≤0.25	2	>128	2	64	≤0.25
4FT	>128	8	0.5	≤0.25	>128	128	>128	64
8GT	>128	16	1	2	>128	128	>128	>128
7FT	>128	16	≤0.25	≤0.25	>128	>128	>128	64
12GT	128	16	0.5	≤0.25	>128	8	128	4
3PT	>128	16	≤0.25	≤0.25	>128	128	>128	64
4FM	128	≤0.25	128	128	>128	>128	>128	>128
5GM	128	≤0.25	8	4	>128	128	>128	>128
5PM	128	≤0.25	32	128	>128	>128	>128	>128
3CM	128	≤0.25	64	128	>128	>128	>128	>128
5CM	128	≤0.25	128	128	>128	>128	>128	>128
4PM	16	≤0.25	4	16	>128	>128	64	≤0.25
11FC	128	≤0.25	0.5	8	>128	16	>128	128
2CC	64	≤0.25	≤0.25	4	>128	4	64	16
10PC	128	≤0.25	≤0.25	4	>128	64	>128	>128
3FC	128	≤0.25	≤0.25	8	>128	128	64	64
12GC	128	≤0.25	≤0.25	4	>128	>128	>128	>128
8GC	>128	0.5	0.5	8	>128	64	128	128
11PC	128	≤0.25	≤0.25	128	>128	32	>128	>128
10GC	128	≤0.25	≤0.25	8	>128	2	>128	≤0.25
11GC	64	1	1	4	>128	128	>128	2
3PC	32	≤0.25	≤0.25	4	>128	64	64	4
3CC	128	≤0.25	≤0.25	128	>128	8	128	32
5PC	128	≤0.25	8	64	>128	128	>128	>128
7CC	128	≤0.25	1	4	>128	128	>128	>128
ATCC 25922	1	≤0.25	≤0.25	≤0.25	8	4	8	≤0.25

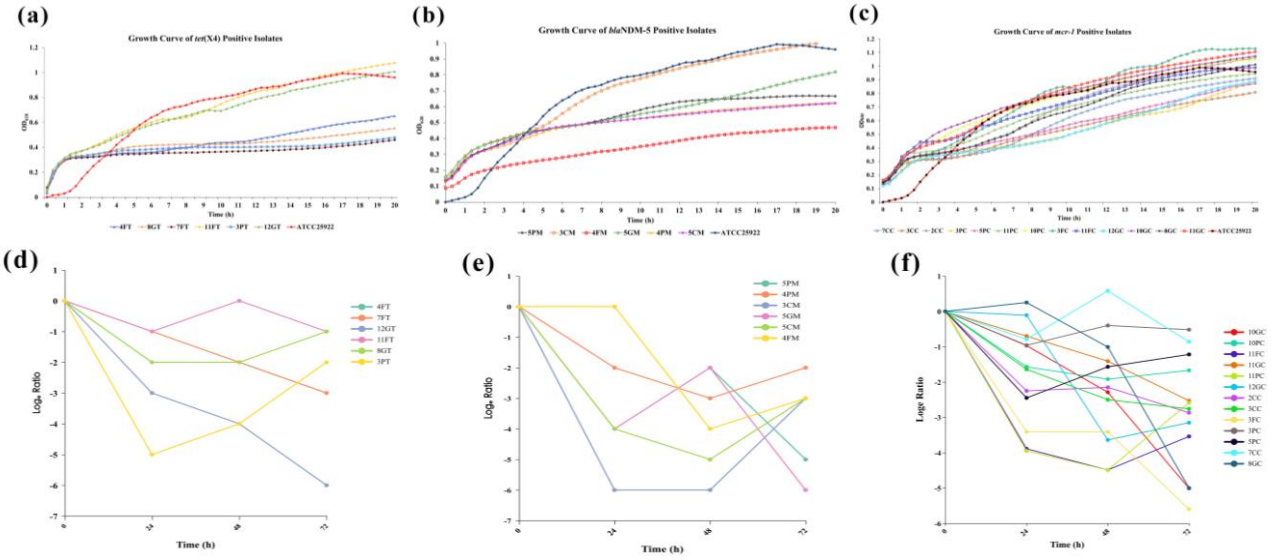

Fig. 2: Growth kinetics and relative fitness costs of resistant *E. coli* isolates. (a–c) Growth curves of *E. coli* isolates carrying *tet*(X4), bla_{NDM-5} and *mcr-1* respectively. Bacterial growth was observed by measuring OD_{600} at indicated time points over a 20-h incubation period. (d–f) Relative fitness of *tet*(X4)-positive (d), bla_{NDM-5}-positive (e), and *mcr-1*-positive (f) isolates, expressed as log fitness ratios compared with the reference strain at 24, 48, and 72 h. Each colored line represents an individual isolate, as indicated in the legends.

Table 3: Conjugation frequencies of bla_{NDM-5} and *mcr-1* positive *E. coli* isolates

Donor Isolate	Resistance profile	Observed Conjugation Frequency	Donor Isolate	Resistance profile	Observed Conjugation Frequency
4FM	bla_{NDM-5}	1.74×10^{-4}	3CC	*mcr-1*	2.00×10^{-4}
3CM	bla_{NDM-5}	6.78×10^{-4}	7CC	*mcr-1*	1.86×10^{-3}
4PM	bla_{NDM-5}	1.2×10^{-3}	3PC	*mcr-1*	2.67×10^{-6}
5CM	bla_{NDM-5}	1.52×10^{-4}	5PC	*mcr-1*	6.25×10^{-4}
5PM	bla_{NDM-5}	1.0×10^{-3}	8GC	*mcr-1*	3.90×10^{-4}
5GM	bla_{NDM-5}	2.06×10^{-3}	10GC	*mcr-1*	3.47×10^{-4}
12GC	*mcr-1*	3.75×10^{-6}	10PC	*mcr-1*	5.29×10^{-4}
3FC	*mcr-1*	2.55×10^{-4}	11PC	*mcr-1*	7.68×10^{-4}
11FC	*mcr-1*	1.17×10^{-3}	11GC	*mcr-1*	6.58×10^{-4}

Phylogenetic analysis and prevalence of ARGs among resistant *E. coli* isolates: A total of 25 resistant *E. coli* isolates were recovered from nine minks (IDs: 2, 3, 4, 5, 7, 8, 10, 11, and 12), with 1–4 isolates per animal, indicating variable colonization patterns. Several minks yielded isolates from multiple anatomical sites, demonstrating within-host dissemination across organ compartments. Mink 11 harbored four isolates from the lungs, spleen, and liver belonging to three sequence types (ST641, ST2165, ST3232), indicating polyclonal colonization. In contrast, mink 5 yielded four isolates from multiple organs, all belonging to ST219, suggesting clonal dissemination. Mink 3 showed high diversity, with isolates from intestine, lungs, and spleen across four STs (ST746, ST346, ST12630, ST1011). Other minks also exhibited either clonal spread (e.g., mink 10, ST641) or multiple lineages within the same or different organs (e.g., mink 4, mink 7, mink 12). Single or limited isolates were recovered from minks 2 and 8 (Fig. 3). Tigecycline resistant *tet*(X4) positive isolates co-carried multiple ARGs including; *floR*, *qnrS1*, *lnu*(G), *aadA22*, bla_{TEM-1}, *dfrA14*, *sul2*, *aph(3'')-Ib*, *aph(6)-Id* and *tet*(A) on nine replicon types: ColE10, Col(pHAD28), ColRNAI, IncFIA, IncFIB, IncFII, IncHI1B, IncHI1A and IncX1 and belong to ST746 and ST2156. Among *tet*(X4)-positive isolates, ST746 predominated and was recovered from lungs (n=2), spleen (n=1), and liver (n=1); ST2165 was isolated from liver and lungs (n=1 each).While bla_{NDM-5} harboring isolates co-carried *mcr-1* and multiple ARGs *aadA2, aadA22, aph(3'')-Ib*, *aph(4'')-Ia, aph(6)-Id*, $bla_{CTX-M-65}$, $bla_{TEM-105}$, *cmlA1*, *erm(B), floR*, *fosA3*, *mdfA, mphA*, *lnu*(f), *oqxA*, *oqxB* , *dfrA14*, *sul1, sul2* and *tet*(A) on IncHI2, IncHI2A, IncFIB, IncFIC, IncB/O/K/Z, IncX3, po111 and pKPC-CAV1321 and colicin family plasmids Col156, Col(MG828), Col(pHAD28) in ST219 (dominant) and ST1011. ST219 was distributed across liver, lungs, spleen, and intestine, most frequently from spleen (n=2); ST1011 occurred only in the intestine. Furthermore, the thirteen colistin resistant *mcr-1* positive isolates carried bla_{CMY-2}, $bla_{TEM-105}$, $bla_{CTX-M-14}$, $bla_{CTX-M-65}$ and *fosA3* on IncFIA, IncFIB, IncFII, IncFIC, IncB/O/K/Z, IncX4, IncI1and IncI2 replicons in nine diverse STs with ST641 (n=4) most common, followed by ST1011. Organ distribution: spleen and liver (n=4 each), intestine (n=3), lungs (n=2) (Fig. 3 and 4B).

All resistant *E. coli* isolates were distributed across phylogroups A, B1, D, E and F. The *tet*(X4)-positive isolates were confined to phylogroups A and B1 carrying ST746 (serotype H37) and ST2165 (serotype H7) respectively. Similarly, the bla_{NDM-5} positive isolates were distributed to D and E phylogroups carrying ST1011 (O160:H16) and ST219 (H34) respectively. Whereas, the *mcr-1* positive isolates shows great diversification with respect to phylogroups and distributed into A, B1, D and F groups belong to diverse STs and serotypes. Phylogroups A and B1 comprised seven isolates each; however, they differed markedly in their ARG profiles. In Phylogroup A *tet(*X4) was predominant than *mcr-1*. In contrast, phylogroup B1 exhibited a predominance of *mcr-1* in comparison to *tet*(X4). All these isolates belong to extraintestinal pathogenic *E. coli* (ExPEC) of the uropathogenic (UPEC) pathotype (Fig. 4A).

The number of SNP differences within *mcr-1*, *tet*(X4), and *bla*NDM-5 positive clones was notably low (0–5, 0–1, and 0–23, respectively) even among isolates recovered from different organs or different animals, suggesting possible clonal relatedness and potential intra-farm dissemination, although definitive conclusions

regarding transmission directionality cannot be drawn in the absence of temporal sampling and epidemiological linkage data (Fig. 4C).

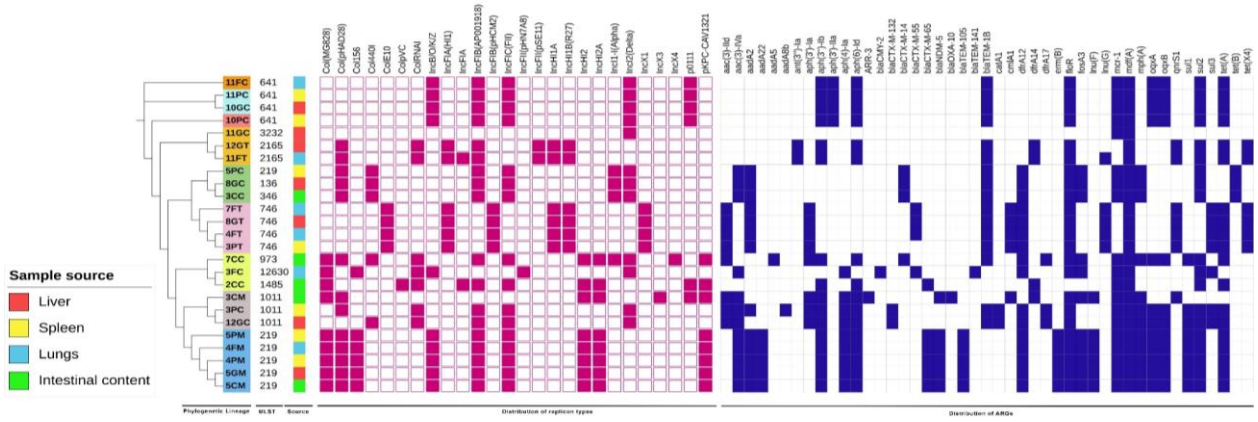

Fig. 3: Phylogenetic relationship of resistant *E. coli* isolates constructed using core genome alignment. Isolate identifiers follow a structured nomenclature where the number denotes the individual mink ID, the first letter indicates the organ site of isolation (C = intestinal content, F = lungs, G = liver, P = spleen), and the second letter indicates the antibiotic used for selective culture (C = colistin, M = meropenem, T = tigecycline). Isolates sharing the same numerical prefix originate from the same individual mink, allowing within-host comparisons across different anatomical sites. Sample source is colour-coded as: red = liver, yellow = spleen, blue = lungs, green = intestinal content. Purple squares indicate the presence of plasmid replicon types and dark blue tiles represent antimicrobial resistance genes (ARGs); white boxes indicate absence. MLST sequence types are annotated for each isolate.

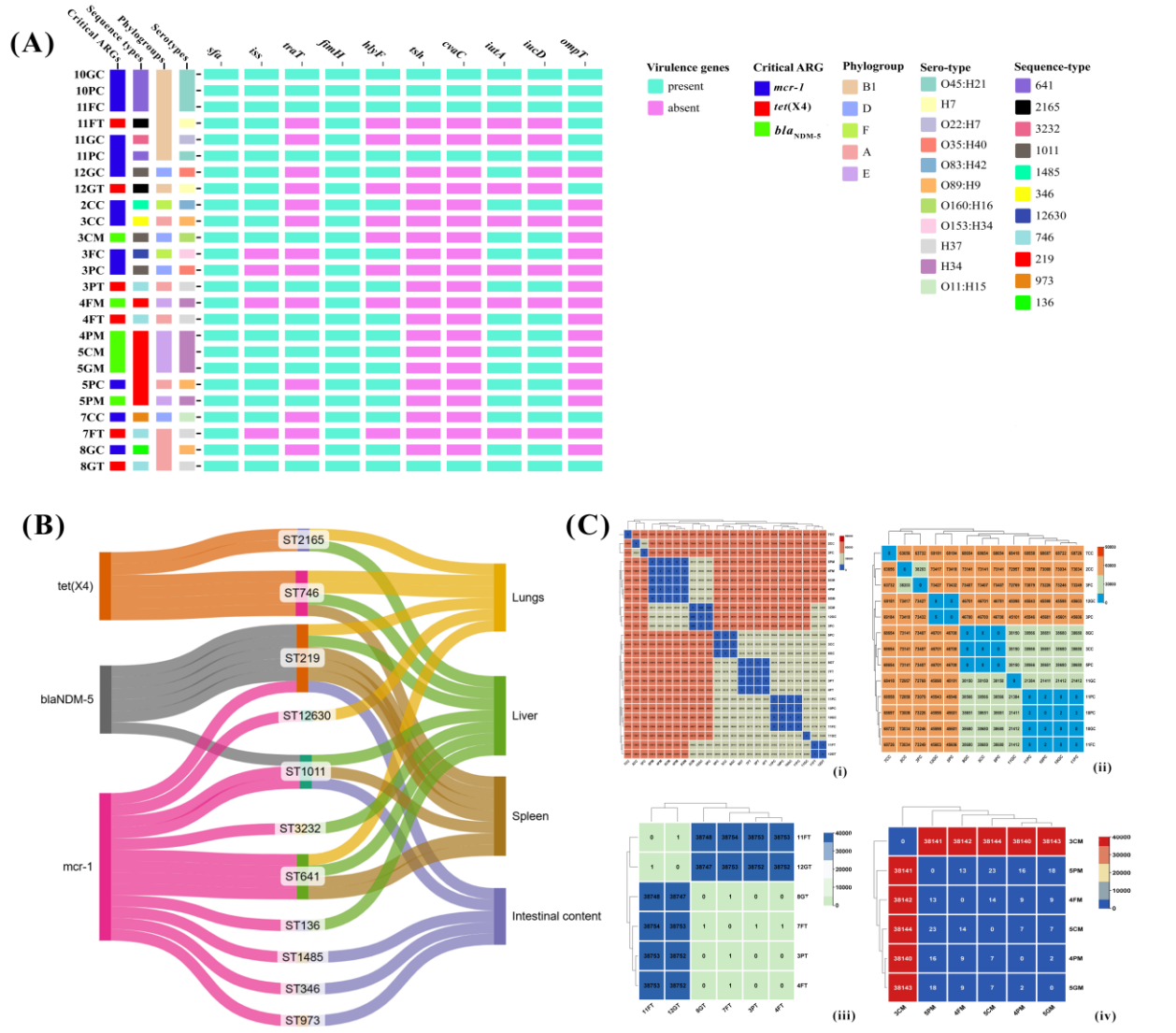

Fig. 4: Genomic characterization and virulence profile of MDR isolates. (A) Heatmap showing distribution of virulence genes (turquoise: present; pink: absent), critical ARGs, phylogroups, serotypes, and STs. (B) Sankey diagram illustrating associations between ARGs, STs, and isolation sources. (C) SNP-based comparative analysis: (i) collective pairwise distance matrix of 25 resistant isolates; (ii–iv) pairwise distance matrices for *mcr-1*, *tet*(X4), and bla_{NDM-5} positive isolates, respectively.

Genomic characterization of *tet*(X4) positive *E. coli* isolates: Two *tet*(X4)-positive isolates 11FT and 3PT were long read sequenced and details regarding the whole genomes are summarized in (Table 1). These isolates harbored the *tet*(X4) gene on a circularized hybrid plasmid of 190,697–190,711 bp, multiple plasmid replicon types (IncFIA (HI1), IncHI1B(R27), and IncHI1A). The presence of multiple replicon types is consistent with a history of plasmid hybridization. This plasmid also co-carried several ARGs such as *floR*, *qnrS1*, *lnu*(G), *aadA22,* and $bla_{\text{TEM-1}}$ and exhibits a high level of similarity to previously sequenced plasmids in the public domain: pTQ2-tetX4 (ON390816.1) with 99.98% identity at 100% coverage, pHN21SC2211TT-tetX4 (OR509737.1) with 99.99% identity at 100% coverage and pE-T306-tetX4 (CP090284.1) with 99.97% identity at 100% coverage. These plasmids were isolated from swine, vegetables and a human respectively. from multiple sources, including swine, vegetables and human respectively (Fig. 5a). While the linear comparison of these two *tet*(X4) bearing plasmid with reference plasmid pF31F2 (PP854072) recovered from swine feces showed that they have same genetic makeup. Comparing our two *tet*(X4) bearing plasmids with the reference plasmid pF31F2 (PP854072) we note that our plasmids contain and IS*1 element* and the *abh* gene that encodes a predicted alpha/beta-hydrolase and is consistently in the conserved hp-*abh*-*tet*(X4) -IS*CR2* region not known to confer tigecycline resistance but helps to mobilize *tet*(X4) gene in plasmids upstream of *tet*(X4) and the insertion sequence IS*CR2* downstream of *tet*(X4). Other virulence genes (e.g. *virD2* and *lysR) and* ARGs (e.g. *qnrS1, floR* and $bla_{\text{TEM-1B)}}$ are also present in our plasmids (Fig. 5b). The presence of the IS elements is consistent with the suggestion that the ARGs may themselves be mobile between different plasmids.

Genomic characterization of $bla_{\text{NDM-5}}$ positive *E. coli* isolates: Two $bla_{\text{NDM-5}}$ carrying *E. coli* isolates, 3CM and 4FM were also long read sequenced to produced closed hybrid assemblies. The bla_{NDM-5} gene was found to be present on a (46,161bp) IncX3 plasmid in isolate 3CM and a (113,155bp) IncB/O/K/Z plasmid in isolate 4FM. These isolates also carry an IncHI2 plasmid that harbors *mcr-1* gene along with multiple other ARGs such as *tet*(A), $bla_{\text{CTX-M-65}}$, $bla_{\text{OXA-10}}$, *floR* (Fig. 8 & Table 1). The $bla_{\text{NDM-5}}$ carrying IncX3 plasmid displays high nucleotide identity and structural conservation with three reference plasmids retrieved from the NCBI database: pNDM-1_IncX3 (CP050161) with 99.99% identity at 100% coverage, pIncX3-103_2 (PQ872734) with 99.99% identity at 100% coverage and pNDM-IncX3I2 (MT621562) with 100% identity and coverage. These reference plasmids were recovered from human rectal swab, ICU and chicken samples respectively. Whereas the linear comparison with pL37-1 (CP034591) another IncX3 plasmid harbored by an

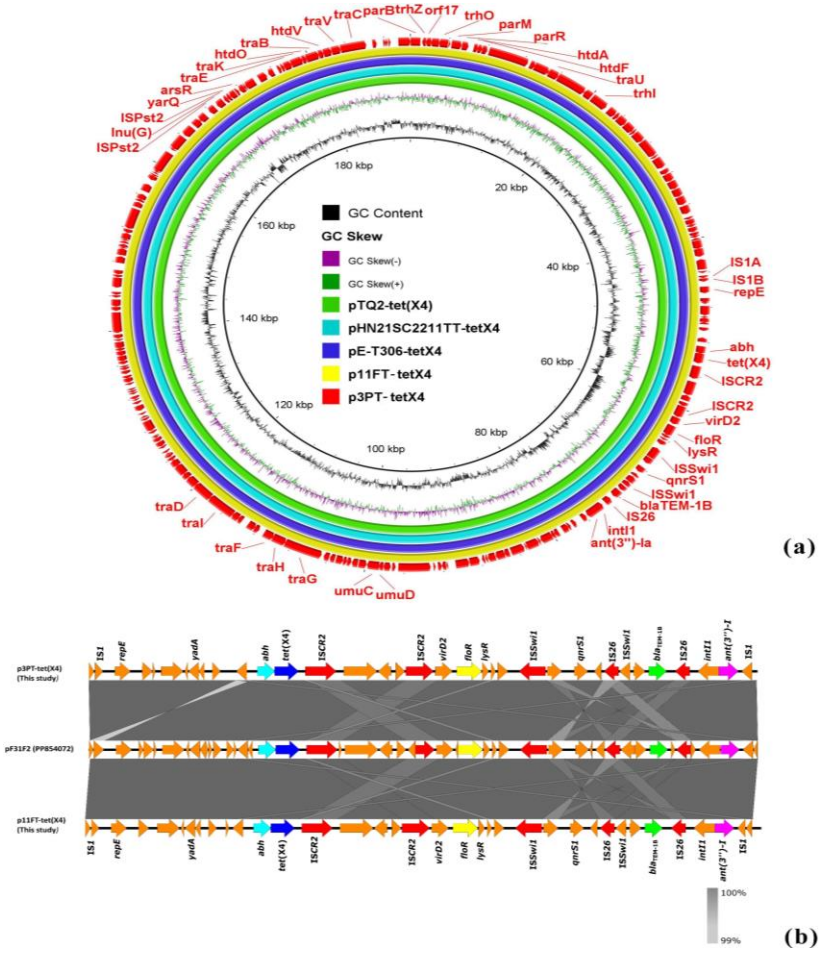

Fig. 5: Circular comparison of five *tet*(X4)-bearing plasmids. (a) Hybrid IncFIA: HI1B:HI1A plasmids p11FT-tetX4 and p3PT-tetX4 were compared with references pTQ2-*tet*(X4), pHN21SC2211TT-tetX4, and pE-T306-tetX4. (b) Genetic context comparison with reference pF31F2 (PP854072) from pork. Colored arrows indicate antimicrobial resistance genes and insertion sequences; gray shading denotes regions of high sequence homology.

isolate recovered from goose exhibit that they have same genetic compartment and IS elements as with IncX3 plasmid harbor by isolate 3CM in our study: IS*5*, IS*Aba125*, IS*3000* and IS*Swi1* upstream of bla_{NDM-5} while bleomycin resistance gene *ble*-$_{MBL}$ and *cutA* downstream to bla_{NDM-5} gene. These elements flank bla_{NDM-5} and are part of a conserved mobile genetic context that facilitates capture and horizontal transfer of the gene between plasmids and bacteria (Fig. 6a).The bla_{NDM-5} positive plasmid IncB/O/K/Z in isolate 4FM also shares a high level of genetic similarity with reference genomes from NCBI database: p1106-NDM (MG825375) 99.73 % identity, pCREC3024-NDM-9_111k (CP191565)with 99.95 % identity, pE-T84-1-NDM-5 (CP090275) with 99.43 % and pL889_NDM9 (MZ062604) with 99.66% identity at 100% coverage These plasmids were recovered from ,multiple sources including chicken and human samples. Similarly, the linear genomic comparison of IncB/O/K/Z plasmid harbor by 4FM with another reference IncB/O/K/Z plasmid pCS18F-NDM-Fos (CP074577) recovered from chicken also showed 99.99% identity and reveal the genetic makeup of bla_{NDM-5} gene that this gene is encounter by IS*26*, and I*SCR1* insertion sequences along with multiple ARGs such as *fosA3*, *dfrA12* and *sul1* upstream while IS*26*, *aph (3)-Ia* and *mph(A)* present downstream to bla_{NDM-5} gene. The same genetic makeup in the competitive genome from different source strengthen this argument that this gene has conserved genetic environment that help in the dissemination of this gene with in plasmids among same or different sources (Fig 6b).

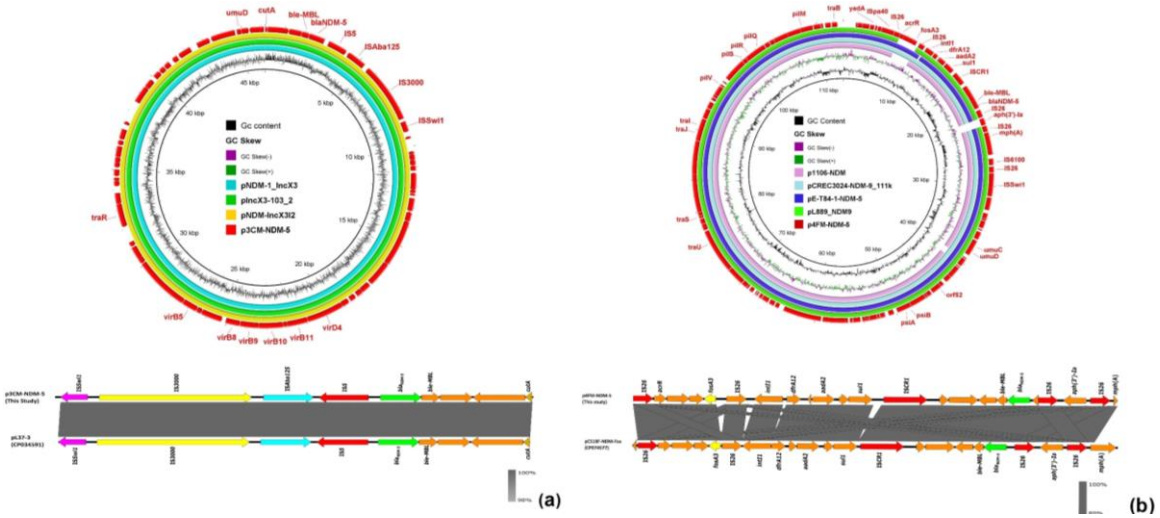

Fig. 6: (a) Circular and linear comparison of IncX3 plasmid p3CM-NDM-5 with references pNDM-1_IncX3, pIncX3-103_2, pNDM-IncX3I2 (circular) and pL37-3 (linear) showing the genetic context of bla_{NDM-5}. **(b)** Circular and linear comparison of IncB/O/K/Z plasmid p4FM-NDM-5 with references p1106-NDM, pCREC3024-NDM-9_111k, pE-T84-1-NDM-5, pL889_NDM9 (circular) and pCS18F-NDM-Fos (linear). Colored arrows indicate antimicrobial resistance genes and insertion sequences; gray shading denotes regions of high sequence homology.

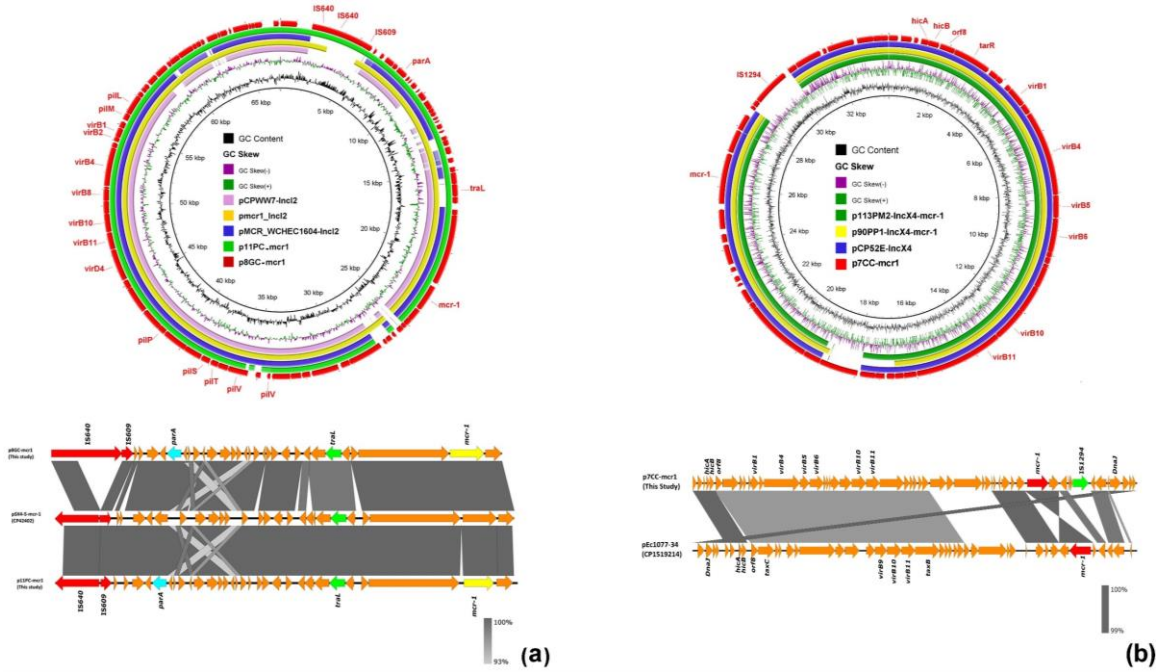

Fig. 7: (a) Circular and linear comparison of IncI2(Delta) plasmids p11PC-mcr1 and p8GC-mcr1 with reference plasmids pCPWW7-IncI2, pmcr1_IncI2, pMCR_WCHEC1604-IncI2 (circular) and pSX4-5-mcr-1 (linear) showing the genetic context of *mcr-1*. **(b)** Circular and linear comparison of IncX4 plasmid p7CC-mcr1 with references p113PM2-IncX4-mcr-1, p90PP1-IncX4-mcr-1, pCP52E-IncX4 (circular) and pEc1077-34 (linear). Colored arrows indicate antimicrobial resistance genes and insertion sequences; gray shading denotes regions of high sequence homology.

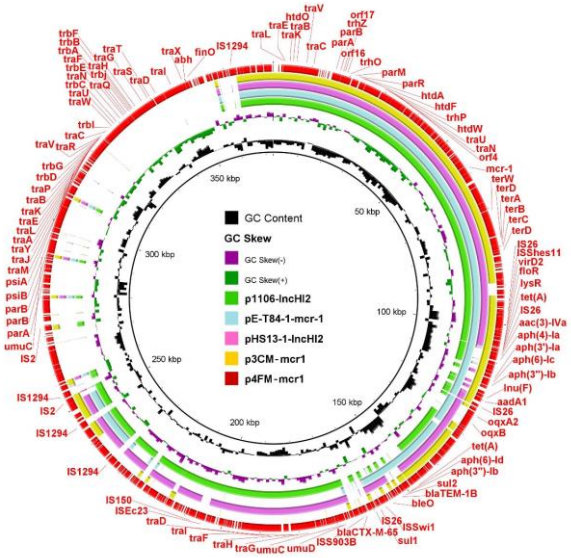

Fig 8: Genomic comparison of *mcr-1* harboring IncHI2 plasmid replicon type named p3CM-mcr1 and p4Fm-mcr1 from this study with three reference plasmids obtained from NCBI databases namely; p1106-IncHI2, pE-T84-1-mcr-1 and pHS13-1-IncHI2.

Genomic characterization of *mcr-1* positive *E. coli* isolates: Three *mcr-1* positive *E. coli* isolates 8GC, 11GC and 7CC subjected to long read sequencing and hybrid assembly (Table 1). Seven replicon types were detected within isolate 7CC including the *mcr-1* harboring IncX4 (~36k) and $bla_{\text{CTX-M-14}}$ and *fosA3* carrying IncHI2 (~230kb). In contrast, isolates 8GC and 11GC carried *mcr-1* gene on a ~67kb and ~68kb IncI2(Delta) plasmid, with 8GC also harboring a 160Kb IncI1-I(Alpha) plasmid carrying $bla_{\text{CTX-M-14}}$ and *fosA3.* The *mcr-1* harboring IncI2(Delta) replicon type from isolate 8GC and 11PC showed high genetic identity with multiple reference genomes; pCPWW7-IncI2 (CP075719), pmcr1_IncI2 (KU761326), pMCR_WCHEC1604-IncI2 (KY829117) (Fig 7A). These reference plasmids were associated with different sources including wastewater and human. Similarly, the linear comparison with and pSX4-5-mcr-1 (CP142402) from sheep showed that they have conserved genetic environment comprises of IS*640* and IS*609* upstream of *mcr-1* gene. While the (Fig. 7b) represent another *mcr-1* positive isolate 7CC that harbor replicon type IncX4 that showed different genetic makeup as it carries only *mcr-1* gene and downstream an IS*1294* that make it diverse from the reference genomes recovered from pig and human samples from NCBI database as they share almost same genetic makeup except this IS*1294* which means that this insertion sequence help this gene to disseminate among this plasmid from environment or other sources via HGT.

DISCUSSION

This is the first report of a plasmid mediated *tet*(X4) gene and the co-occurrence of *mcr-1* and $bla_{\text{NDM-5}}$ genes in *E. coli* isolates recovered from minks in China. This finding is surprising and alarming for public health because these antibiotics are not approved for veterinary use usage, although colistin may have been used as feed additive prior to 2017.

The *tet*(X4)-harboring MDR *E. coli* from minks belong to ST2165 (phylogroup B1, serotype H7) and ST746 (phylogroup A, serotype H37) both frequently reported from diverse hosts and regions. *E. coli* ST746 isolates from mink harboring a ~190kb IncFIA: HI1B(R27):HI1A hybrid plasmid and carrying *tet*(X4) gene, A study from Pakistan similarly reported a hybrid IncFII: IncFIB(AP001918) ~178kb plasmid carrying *tet*(X4) gene harbored by *E. coli* ST746 from wild birds (Mansoor *et al.*, 2024). Moreover, ST746 has also been recovered from wastewater and clinical isolates from South Korea ($bla_{\text{NDM-5}}$), Denmark ($bla_{\text{OXA-48}}$) and China ($bla_{\text{CTX-M-14}}$) (Gedebjerg *et al.*, 2015; Shin *et al.*, 2021; Yang *et al.*, 2022). However, *fosA* positive ST2165 *E. coli* was reported from bovine mastitis and raw milk in Egypt (Tartor *et al.*, 2021); *E. coli* ST2165 (B1, H7) was reported from chickens, raw milk and food-handling utensils in Gambia and Ghana (Foster-Nyarko *et al.*, 2021; Sunmonu *et al.*, 2025), while *mcr-1*-positive *E. coli* ST2165 (B1) was reported from human patient in Italy (Giufrè *et al.*, 2016).The emergence of these clones across human, animal, food, and environmental sources, combined with critical ARGs suggest these clones target for priority One-Health surveillance.

We previously reported $bla_{\text{NDM-5}}$ on ~88-kb IncFII(pHN7A8) plasmid in minks (Munir *et al.*, 2025b). The present study revealed diversification of $bla_{\text{NDM-5}}$ carrying lineages and plasmid in mink-associated *E. coli*: $bla_{\text{NDM-5}}$-was identified on IncX3 plasmid in *E. coli* ST1011, and on IncB/O/K/Z plasmid in ST219 (co-harboring *fosA3*). These $bla_{\text{NDM-5}}$ positive isolates simultaneously harbor *mcr-1* on IncHI2 plasmids along with β-lactamase genes $bla_{\text{OXA-10}}$ and $bla_{\text{CTX-M-65}}$. NDM and *mcr-1*-positive ST1011 is widespread in duck farms (China) and poultry (Lebanon) (Al-Mir *et al.*, 2021; Wang *et al.*, 2021). This clone has also been reported from clinical *mcr* positive isolates from Egypt (Elnahriry *et al.*, 2016) and China (Liang *et al.*, 2021). The detection of *E. coli* ST1011 across ducks, poultry, humans, and minks highlights its broad host range and the co-occurrence of $bla_{\text{NDM-5}}$ and *mcr-1* in mink-derived ST1011 underscores minks as reservoirs for accumulation and dissemination of critical ARGs.

In contrast to *tet*(X4) and $bla_{\text{NDM-5}}$, *mcr-1*–positive *E. coli* is more diverse, corresponding to nine STs (ST641, ST3232, ST219, ST136, ST346, ST973, ST12630, ST1485, and ST101). *E. coli* ST1485 a potential UPEC lineage, circulates across humans, animals, and the environment (Hammad *et al.*, 2022). Its detection in minks (O83:H42) carrying *mcr-1* and $bla_{\text{CTX-M-65}}$ emphasizes farmed minks as reservoirs of high-risk clones. Consistent with this, ST1485 has been reported in humans in Peru co-harboring *mcr-1* and $bla_{\text{CTX-M-55}}$ (Deshpande *et al.*, 2019), and in China from wild animals co-harboring *mcr-1* and $bla_{\text{CTX-M-132}}$ (Lu *et al.*, 2020), highlighting its epidemiological importance and resistance plasticity across the One health interface. Except ST1485 and ST1011, other STs are sparingly reported, yet their recovery with *mcr-1* depicts that colistin resistance is not limited to high-risk clones but can develop across varied *E. coli* lineages in animal reservoirs.

The presence of multiple lineages across organs highlights the ability of resistant *E. coli* to translocate

beyond the GIT and establish infections in systemic sites such as the liver, spleen, and lungs, suggesting possible bacteremia or lymphatic dissemination. Notably, all isolates were classified as ExPEC (Extraintestinal Pathogenic *E. coli*) and UPEC (Uropathogenic E. coli), indicating strong virulence potential mediated by factors such as adhesins, iron acquisition systems, toxins, and immune evasion mechanisms (Fig. 4). The co-occurrence of virulence determinants and MDR genes in these isolates represents a significant clinical concern. Furthermore, the coexistence of diverse sequence types within the same host may facilitate HGT, accelerating the spread of resistance. From a zoonotic perspective, the detection of critical ARGs including *mcr-1*, $bla_{\text{NDM-5}}$, and *tet*(X4), in virulent lineages across multiple organs underscores the role of farmed minks as potential reservoirs of high-risk, multidrug-resistant pathogens with implications for both animal and human health.

Several limitations of this study should be acknowledged. First, sampling was confined to a single fur farm in Shandong Province, which may constrain the generalizability of our findings to other regions or global mink production systems. Yet, Shandong represents one of China's most prominent mink farming areas, thus providing a relevant and representative setting for intensively managed fur production. Second, the cross-sectional design of our study excludes assessment of temporal dynamics or the influence of farm size on resistance gene prevalence. Consequently, future longitudinal surveillance incorporating multiple farms across diverse provinces and seasons is warranted to more fully elucidate the dissemination patterns of these clinically critical resistance. However, the limited documentation of these STs and ARGs probably depicts under-sampling of wildlife and farm niches, highlighting the need for comprehensive One Health surveillance.

Conclusions: To date, this study documented the first report from China indicating the existence of plasmid mediated *tet*(X4) and $bla_{\text{NDM-5}}$ positive isolates co-harboring *mcr-1* gene from minks in China. Resistance plasmids within these *E. coli* isolates have high capability for horizontal distribution, enabling interspecies transmission between livestock and human populations. In accordance with the conserved homologous genetic context of *tet*(X4), and *mcr-1*and $bla_{\text{NDM-5}}$ with respect to humans, food animals and environmental genomes suggest that minks may acts as serve as key vector in the global resistome, harboring ARGs that can be conveyed to humans and livestock. The apparent absence of geographical barriers highlights the role of minks in the environmental persistence of bacterial isolates conferring resistance to last resort antibiotics. Future investigations must prioritize the efficient monitoring of these populations to better comprehend the evolutionary paths and spillover risks linked with emerging resistance factors from One health perspective.

Declarations: Ethics approval and consent to participate Not applicable

Consent for publication: Not applicable.

Availability of data and material: The datasets presented in this study can be found in online repositories NCBI GenBank under https://www.ncbi.nlm.nih.gov/bioproject/PRJNA1395350.

Competing interests: The authors declare that they have no competing interests.

Funding: This work was supported by National Natural Science Foundation of China (12411530085), the Outstanding Youth Foundation of Jiangsu Province of China (BK20231524), National Key Research and Development Program of China (2024YFC3406300) and the Priority Academic Program Development of Jiangsu Higher Education Institutions (PAPD).

Authors contribution: CRediT: AM: Sample processing, data Analysis and draft preparation, and; MS: Visualization and reviewing; YL and RS: Sample collection; EJF: Review and editing; ZW: Funding acquisition; RL: Conceptualization, study design, supervision.

Acknowledgments: Not applicable

Generative AI Statement: The authors used generative AI tools exclusively for language refinement and editing during manuscript preparation. All scientific content, data interpretation, and conclusions were developed by the authors, who take full responsibility for the integrity and accuracy of the work.

REFERENCES

Ahlstrom CA, Woksepp H, Sandegren L, *et al.*, 2022. Genomically diverse carbapenem resistant Enterobacteriaceae from wild birds provide insight into global patterns of spatiotemporal dissemination. Science of the Total Environment 2022;824:153632.

Ahmed ZS, Hashad ME, Atef Y, *et al.*, 2025. Public health threat of antimicrobial resistance and virulence genes in *Escherichia coli* from human-chicken transmission in Egypt. Scientific Reports 15:12627.

Al-Mir H, Osman M, Drapeau A, *et al.*, 2021. WGS analysis of clonal and plasmidic epidemiology of colistin-resistance mediated by *mcr* genes in the poultry sector in Lebanon. Frontiers in Microbiology 12:624194.

Alikhan N-F, Petty NK, Ben Zakour NL, *et al.*, 2011. BLAST Ring Image Generator (BRIG): simple prokaryote genome comparisons. BMC Genomics 12:402.

Beghain J, Bridier-Nahmias A, Le Nagard H, *et al.*, 2018. ClermonTyping: an easy-to-use and accurate in silico method for Escherichia genus strain phylotyping. Microbial Genomics 2018;4(7):e000192.

Bessonov K, Laing C, Robertson J, *et al.*, 2021. ECTyper: in silico *Escherichia coli* serotype and species prediction from raw and assembled whole-genome sequence data. Microbial Genomics 2021;7(12):000728.

Biswas R, Debnath C, Bandyopadhyay S, *et al.*, 2022. One Health approaches adapted in low resource settings to address antimicrobial resistance. Science in One Health 1:100011.

Bolger AM, Lohse M and Usadel B, 2014. Trimmomatic: a flexible trimmer for Illumina sequence data. Bioinformatics 30:2114–2120.

Bortolaia V, Kaas RS, Ruppe E, *et al.*, 2020. ResFinder 4.0 for predictions of phenotypes from genotypes. Journal of Antimicrobial Chemotherapy 75:3491–3500.

Carattoli A and Hasman H, 2020. PlasmidFinder and In Silico pMLST: identification and typing of plasmid replicons in whole-genome sequencing (WGS). Methods in Molecular Biology 2075:285–294.

CLSI, 2020. The clinical and laboratory standards institute subcommittee on Antimicrobial susceptibility testing: Background, organization, functions, and processes.

Dalazen G, Fuentes-Castillo D, Pedroso LG, *et al.*, 2023. CTX-M-producing Escherichia coli ST602 carrying a wide resistome in

South American wild birds: Another pandemic clone of One Health concern. One Health (Amsterdam, Netherlands) 17:100586.

Deshpande LM, Hubler C, Davis AP, *et al*., 2019. Updated prevalence of *mcr*-like genes among *Escherichia coli* and *Klebsiella pneumoniae* in the sentry program and characterization of *mcr-1.11* variant. Antimicrobial Agents and Chemotherapy 2019;63(4):e02450-18.

Elnahriry SS, Khalifa HO, Soliman AM, *et al*., 2016. Emergence of plasmid-mediated colistin resistance gene *mcr-1* in a clinical *Escherichia coli* isolate from Egypt. Antimicrobial Agents and Chemotherapy. 60:3249–3250.

EUCAST, 2024. The european committee on antimicrobial susceptibility testing. Breakpoint tables for interpretation of MICs and zone diameters. Version 14.0, 2024. Http://WwwEucastOrg 0–77.

Foster-Nyarko E, Alikhan NF, Ravi A, *et al*., 2021. Genomic diversity of *Escherichia coli* isolates from backyard chickens and guinea fowl in the gambia. Microbial Genomics 7:1–15.

Gedebjerg A, Hasman H, SØrensen CMø, *et al*., 2015. An OXA-48-producing *Escherichia coli* isolated from a Danish patient with no hospitalization abroad. Infectious Diseases (Auckl) 47:593–595.

Giufrè M, Monaco M, Accogli M, *et al*., 2016. Emergence of the colistin resistance *mcr-1* determinant in commensal *Escherichia coli* from residents of long-term-care facilities in Italy. Journal of Antimicrobial Chemotherapy 71:2329–2331.

Hammad AM, Gonzalez-Escalona N, El Tahan A, *et al*., 2022. Pathogenome comparison and global phylogeny of *Escherichia coli* ST1485 strains. Scientific Reports 12:1–14.

Li R, Lu X, Munir A, *et al*., 2022. Widespread prevalence and molecular epidemiology of *tet*(X4) and *mcr-1* harboring *Escherichia coli* isolated from chickens in Pakistan. Science of the Total Environment 806:150689.

Liang G, Rao Y, Wang S, *et al*., 2021. Co-occurrence of NDM-9 and MCR-1 in a human gut colonized *Escherichia coli* ST1011. Infection and Drug Resistance 14:3011–3017.

Lu X, Xiao X, Liu Y, *et al*., 2020. Widespread prevalence of plasmid-mediated colistin resistance gene *mcr-1* in *Escherichia coli* from Père David's deer in China. mSphere. 2020;5(6):e01221-20.

Lu X, Du Y, Peng K, *et al*., 2022. Coexistence of *tet*(X4), *mcr-1,* and *bla*(NDM-5) in ST6775 *Escherichia coli* Isolates of Animal Origin in China. Microbiology Spectrum 10:e0019622.

Mansoor MH, Lu X, Woksepp H, *et al*., 2024. Detection and genomic characterization of *Klebsiella pneumoniae* and *Escherichia coli* harboring *tet*(X4) in black kites (*Milvus migrans*) in Pakistan. Scientific Reports 14:9054.

Munir A, Li C, Kolenda R, *et al*., 2025a. Exploring the diversity and dissemination dynamics of antimicrobial resistance genes in enterobacteriaceae plasmids across varied ecological niches. Pakistan Veterianry Journal 45:662–672.

Munir A, Lv Y, Song R, *et al*., 2025b. Emergence of carbapenem resistant *Escherichia coli, Morganella morganii*, *Providencia rettgeri* harboring bla_{NDM} genes in minks from China. Veterianry Microbiology 307: 110585.

Overbeek R, Olson R, Pusch GD, *et al*., 2014. The seed and the rapid annotation of microbial genomes using subsystems technology (RAST). Nucleic Acids Research 42:D206-14.

Page AJ, Cummins CA, Hunt M, *et al*., 2015. Roary: rapid large-scale prokaryote pan genome analysis. Bioinformatics 31:3691–3693.

Pakbin B, Brück WM and Rossen JWA, 2021. Virulence factors of enteric pathogenic *Escherichia coli*: A Review. International Journal of Molecular Sciences 2021;22(18):9922.

Peng K, Tong Z, Li C, *et al*., 2025. Rapid reconstruction of multidrug-resistant bacterial genomes using CycloneSEQ nanopore sequencing. iMetaOmics 1–7; 2026;3:e70060.

Poirel L, Madec JY, Lupo A, *et al*., 2018. Antimicrobial resistance in *Escherichia coli*. Microbiology Spectrum 6:10.1128/microbiolspec.arba-0026–2017.

Price MN, Dehal PS and Arkin AP, 2009. FastTree : Computing large minimum evolution trees with profiles instead of a distance matrix. Molecular Biology and Evolution. 2009;26(7):1641-1650.

Prjibelski A, Antipov D, Meleshko D, *et al*., 2020. Using SPAdes De Novo Assembler. Current Protocols in Bioinformatics 70:e102.

Qian J, Wu Z, Zhu Y, *et al*., 2022. One Health: a holistic approach for food safety in livestock. Science in One Health 1:100015.

Ramey AM, 2021. Antimicrobial resistance: Wildlife as indicators of anthropogenic environmental contamination across space and through time. Current Biology 31:R1385–R1387.

Schubert C, Näf J, Petukhov L, *et al*., 2025. Strain-specific galactose utilization by commensal *E. coli* mitigates Salmonella establishment in the gut. PLOS Pathogens 21:1–15.

Seemann T, 2014. Prokka: rapid prokaryotic genome annotation. Bioinformatics 30:2068–2069.

Shin H, Kim Y, Han D, *et al*., 2021. Emergence of high level carbapenem and extensively drug resistant *Escherichia coli* ST746 producing NDM-5 in influent of wastewater treatment plant, Seoul, South Korea. Frontiers in Microbiology 12:1–7.

Sullivan MJ, Petty NK and Beatson SA, 2011. Easyfig: a genome comparison visualizer. Bioinformatics 27:1009–1010.

Sunmonu GT, Adzitey F, Odih EE, *et al*., 2025. Genomic characterization of foodborne Salmonella enterica and *Escherichia coli* isolates from Saboba district and Bolgatanga municipality Ghana. PLoS One 20:1–14.

Tang F, Cai W, Jiang L, *et al*., 2022. Large-scale analysis of fitness cost of *tet*(X4)-positive plasmids in *Escherichia coli*. Frontiers in Cellular and Infection Microbiology 12:1–10.

Tang KWK, Millar BC and Moore JE, 2023. Antimicrobial resistance (AMR). British Journal of Biomedical Science 80:11387.

Tartor YH, Abd El-Aziz NK, Gharieb RMA, *et al*., 2021. Whole-genome sequencing of gram-negative bacteria isolated from bovine mastitis and raw milk: the first emergence of colistin *mcr-10* and fosfomycin *fosA5* resistance genes in *Klebsiella pneumoniae* in Middle East. Frontiers in Microbiology;12:770813.

Vezeau N and Kahn L, 2024. Spread and mitigation of antimicrobial resistance at the wildlife-urban and wildlife-livestock interfaces. Journal of the American Veterinary Medical Association 262:741–747.

Wang MG, Zhang RM, Wang LL, *et al*., 2021. Molecular epidemiology of carbapenemase-producing *Escherichia coli* from duck farms in south-east coastal China. Journal of Antimicrobial Chemotherapy 76:322–329.

Wick RR, Judd LM, Gorrie CL, *et al*., 2017. Unicycler: Resolving bacterial genome assemblies from short and long sequencing reads. PLoS Computational Biology 13:e1005595.

Yang M, Xu G, Ruan Z, *et al*., 2022. Genomic characterization of a multidrug-resistant *Escherichia coli* isolate co-carrying bla_{NDM-5} and $bla_{CTX-M-14}$ genes recovered from a pediatric patient in China. Infection and Drug Resistance15:6405–6412.

Zhang C, Xuan Y, Shan H, *et al*., 2015. Avian influenza virus H9N2 infections in farmed minks. Journal of Virology 12:1–8.